HYScale

D3.1. Assessment of large area AMEL cells

Prepared By:

**CNR
CEA
CENMAT
DLR**

Deliverable Information Sheet

Version	
Grant Agreement Number	101112055
Project Acronym	HYScale
Project Title	HYSCALE – ECONOMIC GREEN HYDROGEN PRODUCTION AT SCALE VIA A NOVEL, CRITICAL RAW MATERIAL FREE, HIGHLY EFFICIENT AND LOW-CAPEX ADVANCED ALKALINE MEMBRANE WATER ELECTROLYSIS TECHNOLOGY
Project Call	HORIZON-JTI-CLEANH2-2022-2
Project Duration	48 months
Deliverable Number	3.1
Deliverable Title	Assessment of large area AMEL cells
Deliverable Type	Report
Deliverable Dissemination Level	PU
Work Package	WP3
Lead Partner	CEA
Authors	Nicola Briguglio (CNR) Antonino Aricò (CNR) Kaveh Moulaee (CNR) Gareth Keeley (CEA) Julien Fage (CENMAT) Schwan Hosseiny (CENMAT) Tobias Morawietz (DLR) Jagoda Chmielarz (DLR)
Contributing Partners	CNR, DLR, CENMAT
Reviewers	CNR, DLR, CENMAT
Official Due Date	30.11.2024
Delivery Date	29.11.2024

History of changes

Version	Date	Description	Author(s)
V1	15.11.2024	Assessment of material performance in small scale cell	Nicola Briguglio (CNR) Kaveh Moulaee (CNR Antonino Aricò (CNR) Gareth Keeley (CEA)
V2	25.11.2024	Assessment of material performance in small scale cell and assessment of large area cell performance	Nicola Briguglio (CNR) Antonino Aricò (CNR) Kaveh Moulaee (CNR) Gareth Keeley (CEA)
V3	29.11.2024	Assessment of material performance in small scale cell and assessment of large area cell performance with durability insights Assessment of stability in small area cell at DLR	Nicola Briguglio (CNR) Antonino Aricò (CNR) Kaveh Moulaee (CNR) Julien Fage (CENMAT) Schwan Hosseiny (CENMAT) Tobias Morawietz (DLR) Jagoda Chmielarz (DLR)

D3.1. Assessment of large area AMEL cells

List of Tables

List of Figures

D3.1. Assessment of large area AMEL cells

Keywords list

- Hydrogen
- Electrolysis
- Anion Exchange membrane
- Stack development
- Materials development
- Renewable energy storage
- Life Cycle Assessment
- Techno Economic Analysis
- System Engineering

Disclaimer

Table of Contents

1. Introduction

The ultimate aim of the HYScale project is the development of a large-area (400 cm²) stack with a power of 100 kW. This requires the upscaling and optimization of membranes, ionomers and electrodes (WP2). In the first eighteen months of the project, WPs 2 and 3 have been working closely together to take this first important step towards achieving the 100 kW stack, i.e. the assembly of a large-area single cell using MEAs based entirely on components produced within the project, and the investigation of their electrochemical performance and stability. This deliverable reports initial results obtained at CNR and DLR using a small single cell, primarily investigating the issue of which material to use as the PTL at the cathode. It goes on to describe findings obtained using the large cell (ca. 400cm²), with which the AionFLX membrane developed at CENmat is compared to the PiperION benchmark (CNR).

2. Optimization of the single cell components for the large area cell

This section outlines the initial phase of component optimization for large-area AMEL cells, focusing on the use of two synthesized catalyst systems provided by CNR and CENmat. The objective of this optimization process is to analyze and enhance the performance of each cell component, e.g. catalysts, membrane, mesh, PTL (porous transport layer), etc., in a small area AEM cell and then to use them as a foundation for scaling up to larger-area AEM cells. These findings will subsequently inform the main goal of this deliverable: achieving effective component and operational optimization for high-performance large-area single cells.

Two types of catalysts were employed in our experiments to assess their influence on cell performance. For cells assembled with CNR catalysts, a synthesized anode catalyst composed of Ni and Fe was utilized, with Pt/C as the cathode catalyst. Both the anode and cathode catalyst-coated substrates (CCS) were prepared through a manual spray-coating process using catalyst ink applied with an airbrush. In figure 1, a schematic sketch of the housing used for the electrochemical test in the small single cell is shown. The active area has a circular shape and the geometrical surface area of the catalyst-coated porous transport layer (PTL + Catalyst= CCS) was maintained at approximately 7.0 cm² to standardize the comparison of the results across various tests.
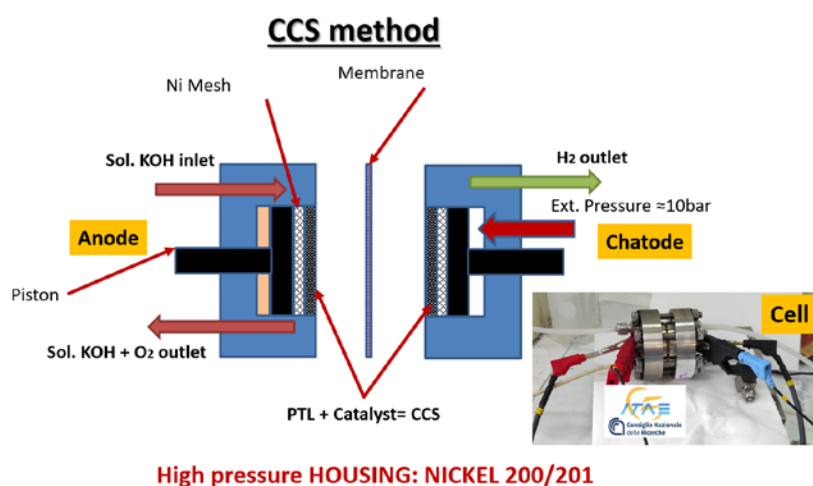
Figure 1. CNR's high pressure housing used for the electrochemical test in small single cell.

The membrane-electrode assembly (MEA) was designed with distinct configurations for each catalyst system. In cells using CNR catalysts, the Fumatech membrane and ionomer were selected to support ionic transport between anode and cathode compartments. For cells based on CENmat catalysts, a different anode catalyst was used to drive the oxygen evolution reaction (OER), paired with a specific cathode catalyst for the hydrogen evolution reaction (HER). CENmat cells incorporated two different membranes, Piperion and AionFLXTM, aiming to evaluate the suitability of each membrane for long-term operation and performance in alkaline environments.

The assembly procedure also differed between these configurations. For CNR-prepared cells, catalyst layers were coated onto the substrates manually at CNR using airbrushing. In contrast, the CCS provided by CENmat came pre-prepared, with the catalyst already deposited onto the Ni felt substrate, ensuring consistency and allowing CNRus to focus exclusively on operational parameters during testing. Electrolyte feeding conditions were standardized with KOH

D3.1. Assessment of large area AMEL cells

solutions of two concentrations, 0.1 M and 1 M, introduced on the anode side, while the cathode side was run without circulating KOH.

The findings from these tests, using small-area AEM single cell, will contribute to identifying the optimum materials, membrane, PTL thickness and other AEM electrolyser components, and operational conditions for large-area single cells.

2.1 Studies using CNR catalysts at CNR

To investigate the optimized conditions by using CNR catalysts, we assembled and tested two small-area cell configurations, both fed with a 1 M KOH solution on the anode side. The aim was to examine the impact of different porous transport layers (PTLs) on cell performance, specifically comparing the behavior when using Ni felt supplied by the project partner Bekaert (450 µm thickness) on the anode side with two different cathode configurations: one using carbon paper as the PTL (with Pt/C deposited) and the other employing Ni felt (450 µm) for both the anode and cathode sides (table 1).

Table 1. CNR cell configurations with CNR catalysts

Cell configuration				
	Catalyst/Material	**Loading/thickness**	**Ionomer**	**PTL**
Anode	NiFe (CNR)	2.2 mg/cm^2	Fumatech (commercial)	Nickel felt 450 µm (Bekaert)/Carbon paper 450 µm
Cathode	Pt/C (CNR)	1.0 mg/cm^2	Fumatech (commercial)	Nickel felt 450 µm (Bekaert)
AEM Membrane	Fumatech (commercial)	50 µm	/	/

- **Polarization curves**

Figure 2 presents the polarization curves for the two cell configurations, with the red curve representing the Ni felt (450 µm) anode and carbon paper cathode setup, and the blue curve showing the results for the cell with Ni felt (450 µm) on both the anode and cathode. The tests were conducted at a KOH concentration of 1 M.

D3.1. Assessment of large area AMEL cells
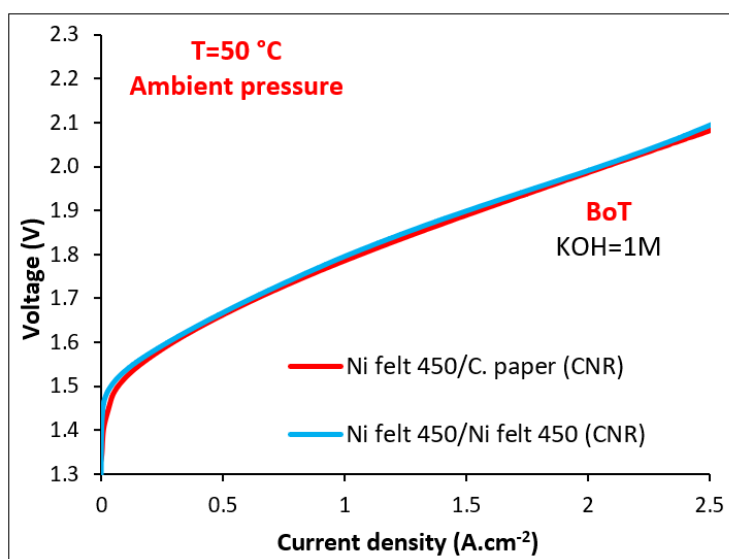
Figure 2. Polarization curves at CNR for two cell configurations in which Ni felt with thickness of 450 µm was used as anode PTL and cathode PTL was carbon paper (red), and Ni felt 450 µm was used at both anode and cathode (blue). For both cell configurations anode electrocatalyst was Ni-Fe CNR catalyst and cathode catalyst was Pt/C. Polarization curves were obtained just after electrochemical conditioning (beginning of the test=BoT)

Based on these polarization curves, both configurations demonstrated very similar performance. The close alignment in performance suggests that both configurations can effectively support the electrochemical processes in the cell.

- **Electrochemical impedance spectroscopy**

To further understand the electrochemical behavior of these configurations, potentiostatic EIS measurements were conducted at two different applied cell voltages: 1.5 V and 1.8 V. Figures 3a and 3b compare the impedance spectra of the two configurations at each potential.

The EIS data indicate that the cell configuration with Ni felt on both anode and cathode sides exhibits higher overall cell resistance compared to the configuration with carbon paper as the cathode PTL.

This increased cell resistance could be attributed to the structural and morphological properties of the Ni felt, which may introduce greater ohmic resistance due to its thickness and material characteristics. However, the Ni felt/Ni felt configuration showed a lower charge transfer resistance, suggesting improved catalytic activity at the electrode-electrolyte interface.

D3.1. Assessment of large area AMEL cells
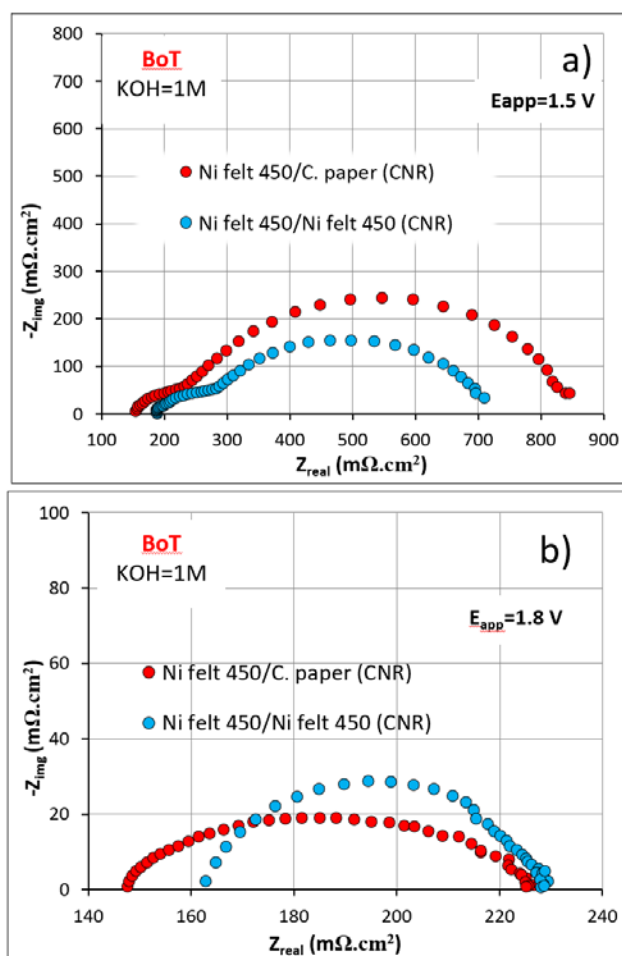
Figure 3. Electrochemical impedance spectroscopy analyses at CNR for two cell configurations in which Ni felt with thickness of 450 μm was used as anode PTL and cathode PTL were carbon paper (red) and Ni felt 450 μm (blue). For both cell configurations anode electrocatalyst was Ni-Fe CNR catalyst and cathode catalyst was Pt/C. EIS data were obtained at three different applied potentials of a) 1.5 V and b) 1.8 V just after electrochemical conditioning (beginning of the test=BoT).

These findings indicate that while the Ni felt/Ni felt configuration may introduce additional resistive elements within the cell, it may simultaneously facilitate charge transfer processes, a balance that could be beneficial in specific operational conditions or cell designs. The overall effect will compensate each other and finally we have observed a similar behavior when we consider polarization curves.

2.2 Studies using CENmat catalysts at CNR

We explore the performance of small-area single cells assembled with CENmat catalysts. For these cells, both the anode and cathode catalyst-coated substrates (CCS) were utilized as received, with catalysts pre-deposited onto the porous transport layers (PTLs). We tested two configurations: one employing Ni felt (450 μm, supplied by the project partner Bekaert) as the CCS on both the anode and cathode sides, and the other using Ni felt (450 μm) as the anode CCS while the cathode was configured with carbon paper.

For the CENmat cells, the cells whose CCS and membrane were received from CENmat, Piperion and AionFLX™ (manufactured by CENmat) with a thickness of 60 and 80 μm, respectively, were employed as the anion exchange membrane (table 2). Polarization curves were extracted from chronopotentiometry analysis conducted at various applied current

D3.1. Assessment of large area AMEL cells

densities, ranging from 0.0075 to 2 A cm⁻². In accordance with CENmat protocol, galvanostatic electrochemical impedance spectroscopy at three applied current densities of 0.025, 0.1 and 1 A.cm^{-2} was carried out. However, only the most significant results are shown in the EIS plots (fig. 4)

Table 2. CNR cell configurations with CENmat's and Bekaert's components.

Cell configurations				
	Catalyst/Material	**Loading/thickness**	**Ionomer**	**PTL**
Anode	OXYGN-N (CENmat)	Confidential (CENmat)	AionFLX™ (CENmat)	Nickel felt 450 µm (Bekaert)/Carbon paper 450 µm
Cathode	H2GEN-M (CENmat)	Confidential (CENmat)	AionFLX™ (CENmat)	Nickel felt 450 µm (Bekaert)
AEM Membrane	Piperion (commercial)	60 µm	/	/

- **Polarization curves**

The polarization curves indicate that the configuration with carbon paper as the cathode CCS exhibits superior performance compared to the Ni felt/Ni felt configuration, particularly at higher current densities in KOH 1 M (figure 4).
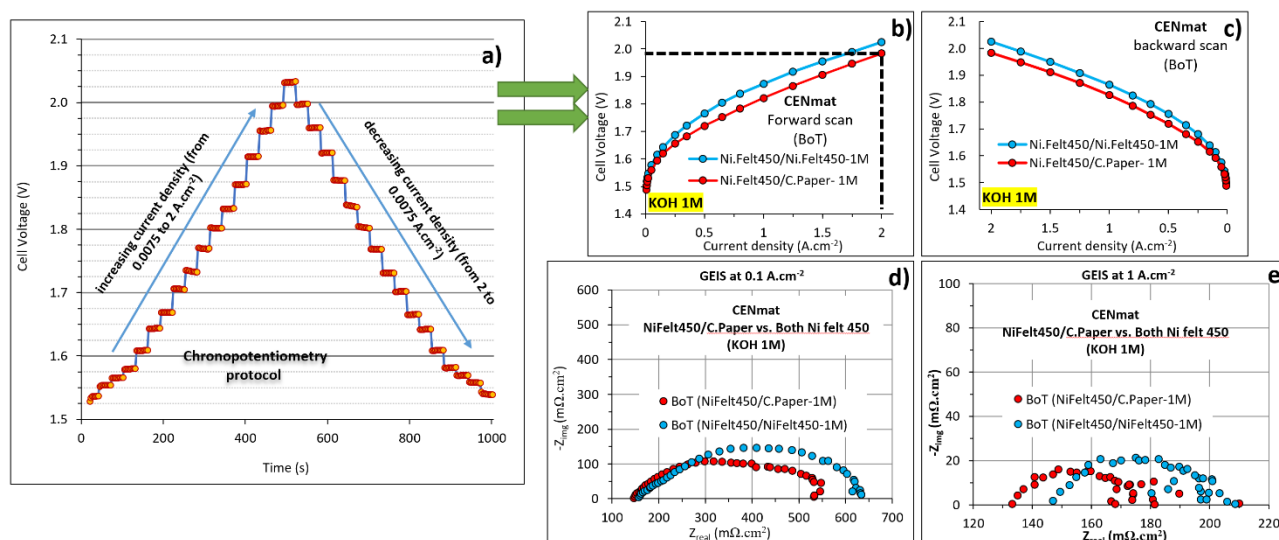
Figure 4. a) Chronopotentiometry protocol and related polarisation curves for forward current steps (b) and backward current steps (c) in KOH 1 M. Dwelling time at each current density step was 30 seconds and the last points were extracted and considered as the cell voltage at that applied current density. d) and e) galvanostatic EIS performed at current densities of 0.1 and 1 A.cm^{-2}.

Figure 4b shows a performance of 1.98 V at 2 A/cm^2 using materials developed in the project. This demonstrates the achievement of the Milestone 3a (2A/cm^2 at Ecell <1.85-2 V/cell). The EIS data at higher current densities and low frequency is quite noisy. The effect can arise from capacitive phenomena (e.g., variations in the double layer, membrane-catalyst coupling), inductive effects (e.g., parasitic inductance from cables or the electrochemical system, including membrane-catalyst interactions), and transient phenomena such as gas bubble formation (fig.4 e).

D3.1. Assessment of large area AMEL cells

- **Galvanostatic EIS**

To further evaluate the electrochemical behavior of the CENmat catalyst configurations, we conducted EIS measurements on both cell setups: one with Ni felt (450 µm) as the CCS on both anode and cathode sides, and the other with Ni felt on the anode side and carbon paper as the cathode CCS. These analyses provide insights into the resistive and charge transfer characteristics associated with each configuration. Figures 4d and 4e show the potentiostatic EIS results for the two configurations, highlighting differences in cell resistance and charge transfer resistance. For the configuration with carbon paper as the cathode CCS, both the cell resistance (evident at the higher frequency end of the EIS plot) and the charge transfer resistance are lower compared to the Ni felt/Ni felt configuration. This lower resistance in the carbon paper configuration aligns with the polarization curve results, where the carbon paper-supported cell showed better initial performance.

Furthermore, short-term stability tests conducted at an applied current density of 1 A cm⁻² indicated that the Ni felt/Ni felt configuration offers superior stability, see figure 5. After 3 days of continuous operation, cells with Ni felt on both sides retained a more stable performance profile, whereas the configuration with carbon paper on the cathode exhibited significant performance degradation. This stability advantage supports the choice of Ni felt for both sides, as it is essential to maintain consistent cell performance over extended periods, especially in stack applications.

D3.1. Assessment of large area AMEL cells
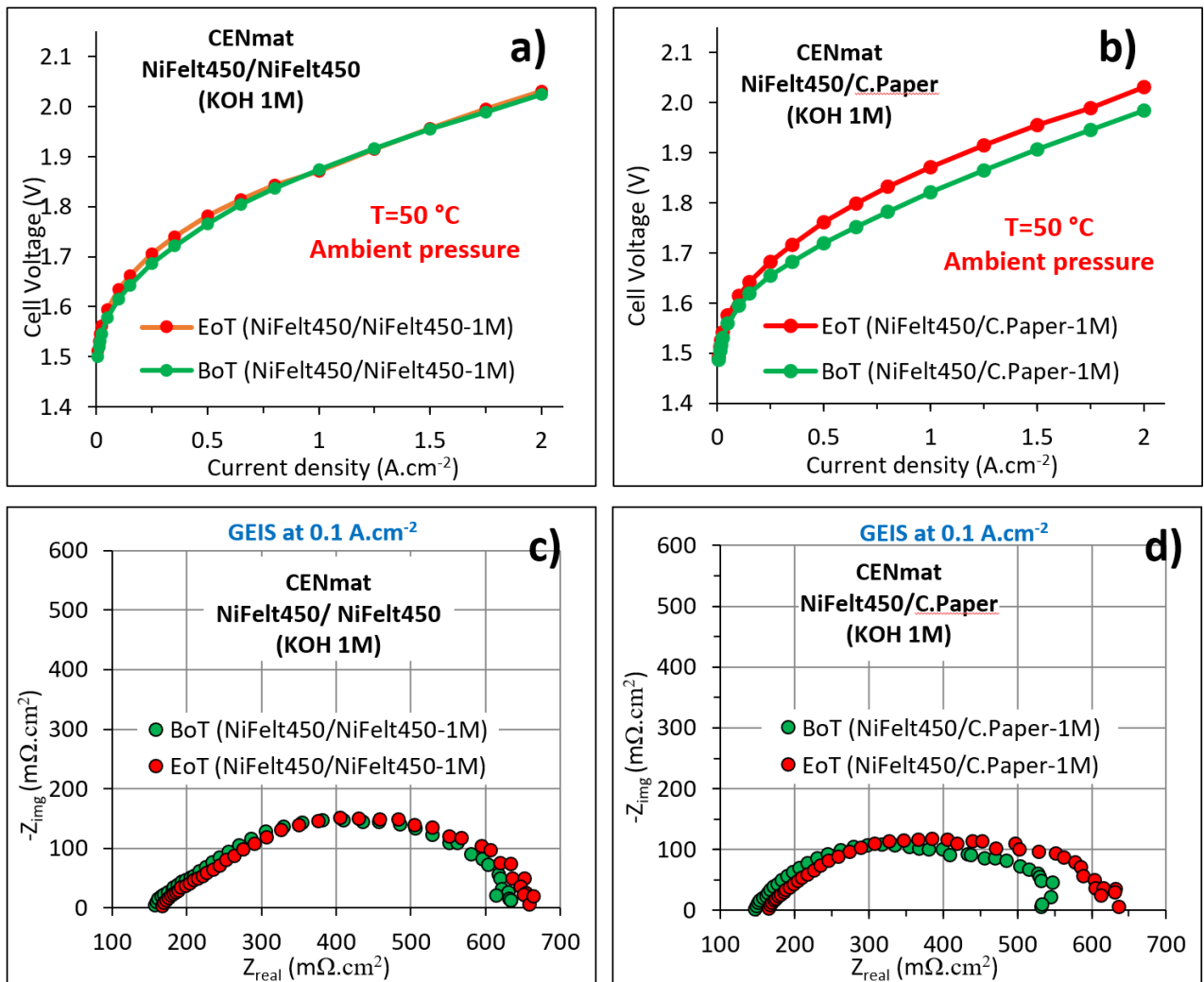
Figure 5. Polarization curves (a and b) and galvanostatic EIS (c and d) graphs at CNR of two cell configurations at BoT and EoT. Applied current density was 1 A.cm^{-2} and KOH= 1 M.

In addition, since Ni felt has a higher mechanical strength compared to carbon paper, it offers added structural stability, which is particularly important for stack designs where mechanical durability is critical. Additionally, a symmetrical design, using Ni felt on both the anode and cathode sides, is generally more favorable for stack integration, as it can simplify the assembly process and improve uniformity across multiple cells in a stack.

In summary, while the carbon paper-based cathode configuration demonstrated an initial performance advantage, the Ni felt/Ni felt configuration was selected to meet the structural and operational requirements for large-area cells. The greater mechanical strength and enhanced stability of Ni felt ensure that this configuration is better suited for long-term, high-demand applications, aligning with the project's goals for stack development.

2.3 Performance comparison at CNR for CENmat cells with Piperion membrane: KOH 0.1 M vs. KOH 1 M

Following our decision to proceed with a cell configuration using Ni felt (450 µm) on both the anode and cathode sides, we conducted a comparative analysis to assess performance differences when using KOH electrolyte concentrations of 0.1 M and 1 M (table 3). This comparison, evaluated at both the beginning of the test (BoT) and end of the test (EoT),

D3.1. Assessment of large area AMEL cells

includes polarization and galvanostatic electrochemical impedance spectroscopy (GEIS) data, as well as a short stability testing under a constant applied current density, see figure 6. In detail, the short stability test highlights a more stable behavior of the cell in a 1 M KOH solution compared to a 0.1 M KOH solution. It is likely that the cell operating at the lower KOH concentration requires additional time to achieve stable conditions (fig. 6e).

Table 3. CNR cell configurations with CENmat's and Bekaert's components.

Cell configurations				
	Catalysts	**Loading/thickness**	**Ionomer**	**PTL**
Anode	OXYGN-N (CENmat)	Confidential (CENmat)	AionFLX™ (CENmat)	Nickel felt 450 µm (Bekaert)
Cathode	H2GEN-M (CENmat)	Confidential (CENmat)	AionFLX™ (CENmat)	Nickel felt 450 µm (Bekaert)
AEM Membrane	Piperion (commercial)	60 µm	/	/

- **Polarization curves**

Figures 6a and 6b illustrate the polarization curves for the Ni felt/Ni felt configuration in KOH 0.1 M and 1 M at BoT and EoT, respectively. The data indicate that the cell operating with KOH 1 M consistently outperforms the cell with 0.1 M KOH. In 1 M KOH, a lower cell voltage is required to reach a given current density, which signifies enhanced cell efficiency and lower overpotential requirements across the operational range. This improvement can be attributed to the higher ionic conductivity provided by the increased KOH concentration, which enhances ion transport and reduces resistance within the cell.

- **Galvanostatic EIS**

Figures 6c and 6d present GEIS measurements at a current density of 0.1 A cm^{-2}. The EIS data further support the polarization observations, as the cell in 1 M KOH shows lower cell resistance compared to that in 0.1 M KOH. The higher KOH concentration reduces ohmic losses and enhances the overall ionic conductivity of the electrolyte, leading to improved charge transfer kinetics and decreased resistance at the electrode-electrolyte interfaces.

D3.1. Assessment of large area AMEL cells
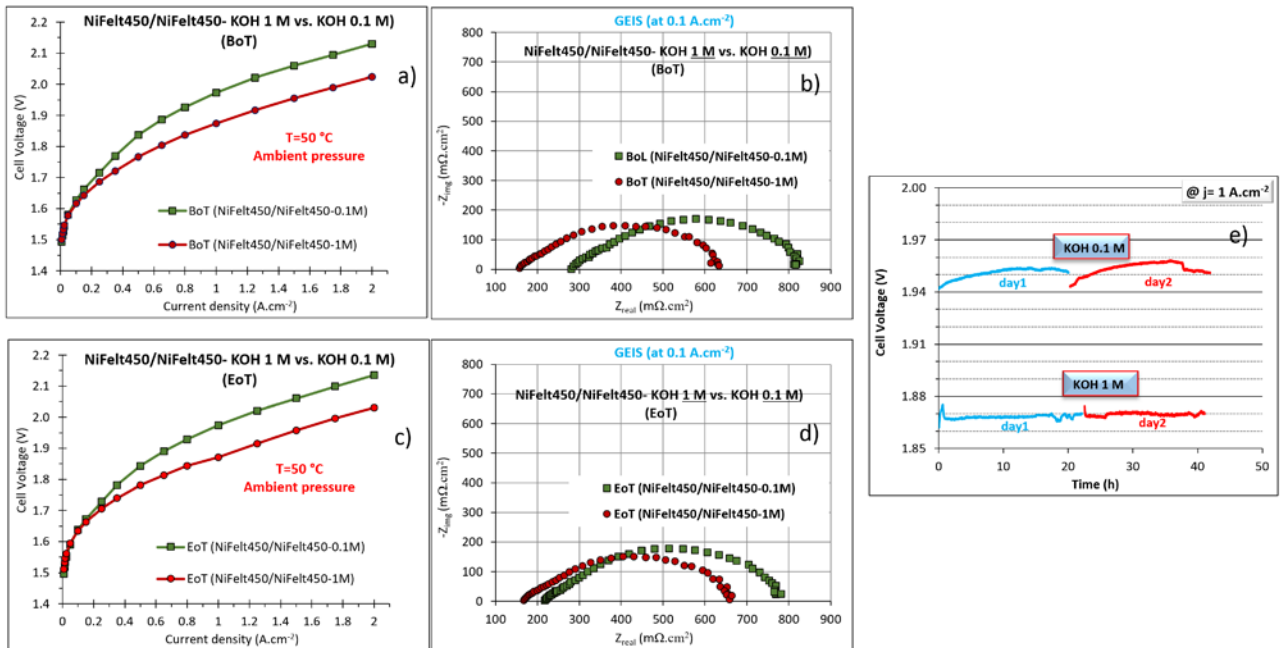
Figure 6. Performance comparison at CNR in KOH 1 M vs. KOH 0.1 M. a and b polarisation curves at BoT and EoT in two different concentrations of KOH. C and d correspond GEIS for KOH 1 M and 0.1 M BoT and EoT; e) short stability test at 1 A/cm^2.

- **Short-term Stability testing at CNR**

Figure 6e provides chrono-potentiometry stability results for both configurations at an applied current density of 1 A cm^{-2}. Over the course of a 2-day stability test, the cell operating in KOH 1 M demonstrates greater stability and a more consistent performance profile, while the cell in KOH 0.1 M experiences a higher degree of voltage drift. The increased stability observed with 1 M KOH further suggests that the higher concentration better supports the cell's requirements for ion conduction and minimizes polarization losses, resulting in a more robust operational stability.

The enhanced performance observed with 1 M KOH can be attributed to several factors:

- *Increased Ionic Conductivity:* A higher concentration of KOH increases the availability of OH$^-$ ions, which accelerates ionic transport across the membrane and reduces overall cell resistance. This improved conductivity enables the cell to operate more efficiently, particularly at higher current densities.
- *Lower Electrolyte Resistance:* The increased ion concentration in 1 M KOH reduces the internal ohmic resistance, which is reflected in the lower cell voltage required to reach a specific current density and the decreased resistance observed in the GEIS data.
- *Improved Charge Transfer:* Higher KOH concentration may facilitate better electrode kinetics for the oxygen evolution reaction (OER) at the anode and the hydrogen evolution reaction (HER) at the cathode. This improvement can contribute to lower charge transfer resistance, as indicated by the EIS data, which allows for more efficient reactions at the electrode surfaces.

D3.1. Assessment of large area AMEL cells

2.4 Performance comparison at CNR for CENmat cells with AionFLX ™ membrane: KOH 0.1 M vs. KOH 1 M

To further explore performance optimization, we conducted a comparative analysis using a new membrane and ionomer, AionFLX™, supplied by CENmat (table 4). With a thickness of 80 μm, AionFLX™ was employed in place of the Piperion membrane, alongside CENmat-provided HER and OER catalyst-coated substrates (CCS) that were chemically and electrochemically conditioned prior to testing. This section evaluates the polarization and galvanic electrochemical impedance spectroscopy (GEIS) data for cells operating in KOH concentrations of 0.1 M and 1 M.

Table 4. CNR cell configurations with CENmat´s and Bekaert´s components.

Cell configurations				
	Catalysts	**Loading/thickness**	**Ionomer**	**PTL**
Anode	OXYGN-N (CENmat)	Confidential (CENmat)	AionFLX™ (CENmat)	Nickel felt 450 μm (Bekaert)
Cathode	H2GEN-M (CENmat)	Confidential (CENmat)	AionFLX™ (CENmat)	Nickel felt 450 μm (Bekaert)
AEM Membrane	AionFLX (CENmat)	80 μm	/	/

- **Polarization Curves**

Figures 7a and 7b display the polarization curves for the AionFLX ™ membrane cell configuration at the beginning of the test (BoT) for 1 M and 0.1 M KOH. In Figure 7a, polarization data from a forward ramp of current densities were recorded during chronopotentiometry analysis, while Figure 7b represents the reverse (backward) scan of current densities. As observed with the Piperion membrane, the AionFLX ™ cell configuration operating with 1 M KOH shows a lower cell voltage across a range of current densities. This lower voltage at each current density indicates improved performance when using the higher concentration, suggesting that 1 M KOH better supports efficient ion transport and lower overpotentials, in line with previous observations.

- **Galvanostatic EIS**

Figures 7c and 7d illustrate the GEIS data comparing cell resistance in 1 M and 0.1 M KOH concentrations, recorded at BoT. Measurements were conducted at two distinct current densities: 0.025 A cm^{-2} (Figure 7c) and 0.1 A cm^{-2} (Figure 7d). In both cases, the cell operating in 1 M KOH exhibits a reduced cell resistance, as shown by the lower intercept of the EIS graph with the real axis (Z_{real}) at higher frequencies. This lower cell resistance observed at 1 M KOH indicates a more efficient ion-conducting pathway within the AionFLX™ membrane, resulting in diminished ohmic and charge transfer losses.
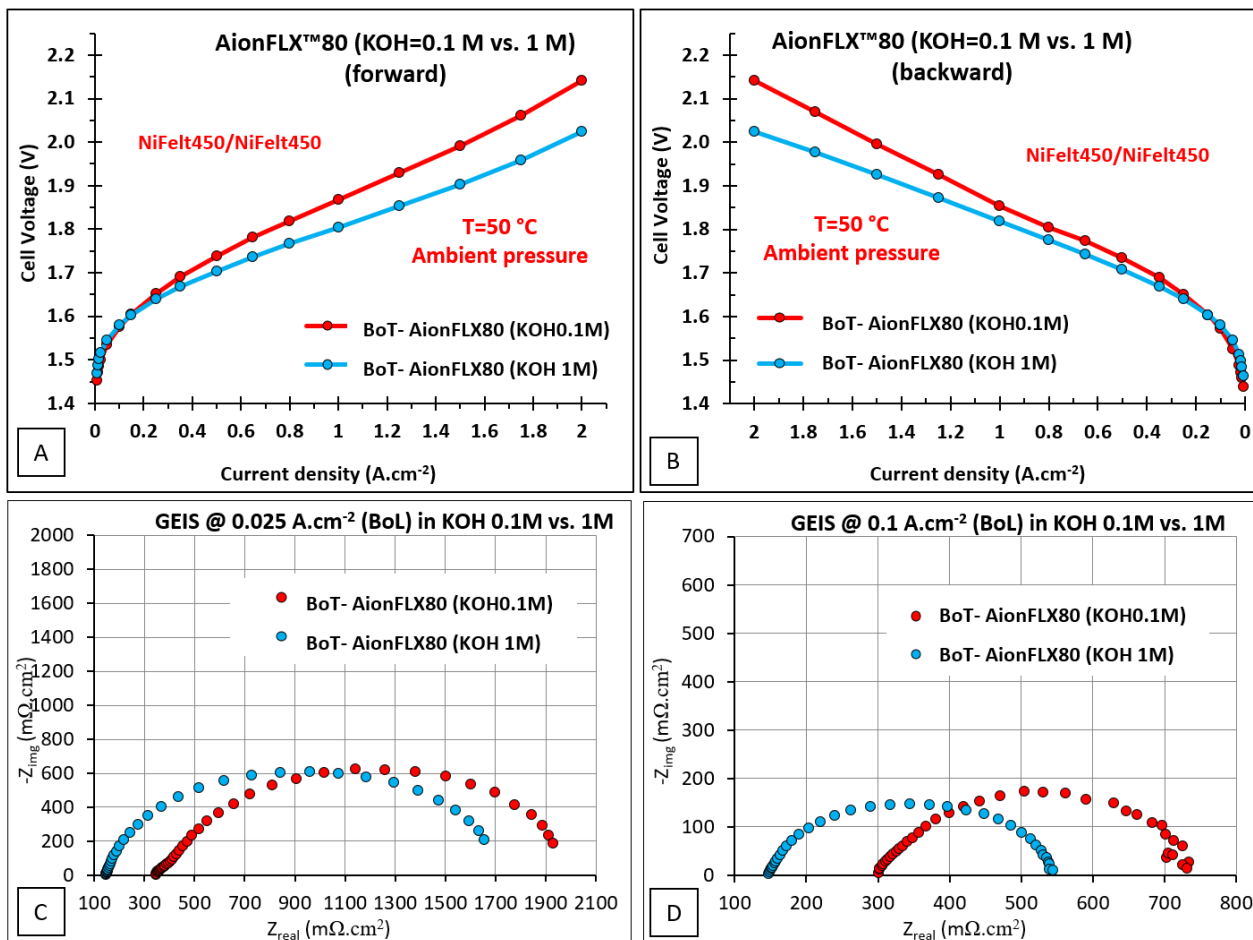
Figure 7. Polarization curves comparing cell assembled using AnioFLX membrane and ionomer in KOH 1M and 0.1 M for forward scan of the current densities, i.e. from 0.0075 to 2 A.cm-2 (a) and backward scan from 2 to 0.0075 Acm-2 (b) Galvanostatic electrochemical impedance spectroscopy at applied current density of (c) 0.025 and (d) 0.1 Acm-2 in KOH 1 and 0.1 M. All data shown here are collected at the BoT of the cell (CNR).

- **Comparative insights**

The performance trends for cells using the AionFLX™ membrane parallel those observed with Piperion. The cell in 1 M KOH consistently demonstrates lower cell voltages and resistances, suggesting that the AionFLX™ membrane also benefits from a higher electrolyte concentration to facilitate optimal ion conduction and efficient charge transfer at both current densities.

2.5 Comparative performance analysis at CNR of Piperion and AionFLX™ membranes

We compared the initial performance of two anion exchange membranes (AEMs)—Piperion and AionFLX—at KOH concentrations of 1 M and 0.1 M. Polarization curves and electrochemical impedance spectroscopy (GEIS) measurements provide insights into the initial performance at the beginning of the test (BoT).

- **Polarization Curves**

Figures 8b and 8d show the polarization curves for cells assembled with Piperion and AionFLX membranes at BoT. When operated in 1 M KOH (Figure 8d), the AionFLX membrane demonstrates a notable performance advantage over the Piperion membrane, especially at low and intermediate current densities, where it consistently achieves lower cell voltages. This

D3.1. Assessment of large area AMEL cells

trend is also observed in 0.1 M KOH (Figure 8b), where the AionFLX configuration again outperforms the Piperion cell, indicating that the AionFLX membrane facilitates better ion conductivity and charge transfer across a range of operating conditions. At higher current densities, however, the performances of the two membranes converge, suggesting that factors beyond membrane type, such as diffusion limitations, may influence performance in this region.

- **GEIS Analysis**

Supporting the polarization data, GEIS measurements reveal that the AionFLX membrane exhibits a lower charge transfer resistance at both KOH concentrations, as indicated by the reduced semicircle diameter in the EIS Nyquist plots (fig 8a, 8c). This lower charge transfer resistance for AionFLX likely contributes to its superior initial performance at BoT. Lower charge transfer resistance suggests enhanced reaction kinetics at both electrodes, allowing the cell to achieve a given current density with lower overpotentials.
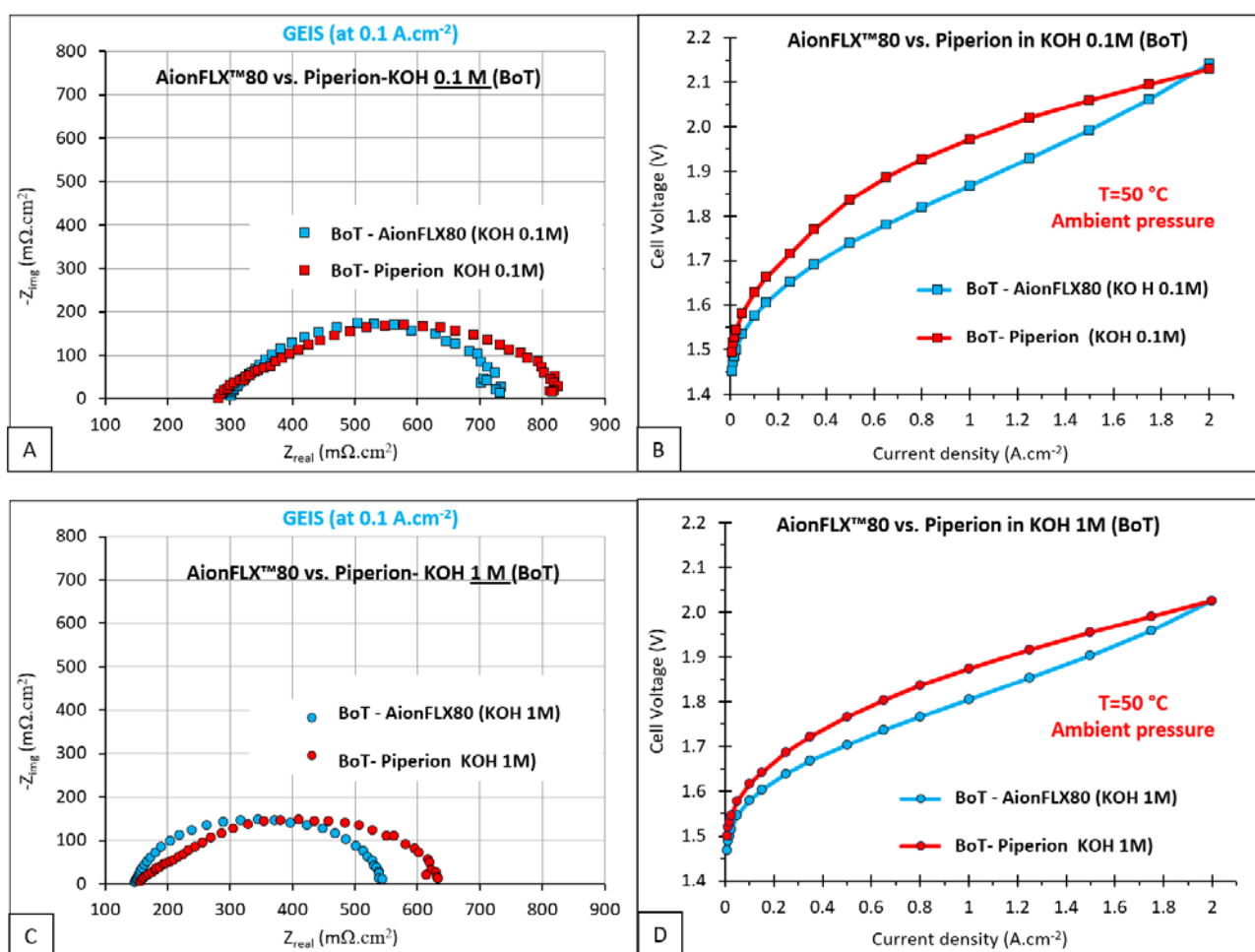
Figure 8. Performance comparison of AionFLX membrane and Piper ionomer in KOH 1M and 0.1 M. a and b polarization curves c and d galvanostatic impedance spectroscopy at applied current density of 0.1 A.cm^{-2}.

2.6 Performance at DLR for CENmat cells with AionFLX ™ membrane

The performance of AionFLX membrane with CENmat catalysts on Bekaert PTLs in 0.1 M KOH at 50 °C was in addition evaluated at DLR. The performance target was nearly reached with 2.01 A cm^{-2} at 2.01 V. The performance curve, using the harmonized EU protocol is shown in Figure 9.

D3.1. Assessment of large area AMEL cells

Figure 9. Performance of AionFLX membrane in 0.1 M KOH and 50 °C.

2.7 Durability measurement at DLR for CENmat cells with AionFLX ™ membrane

The durability of the CENmat cells including AionFLX membrane and CENMat catalyst for both anode and cathode on Bekaert PTLs using nickel endplates was performed for small area cells (4 cm²) at DLR.
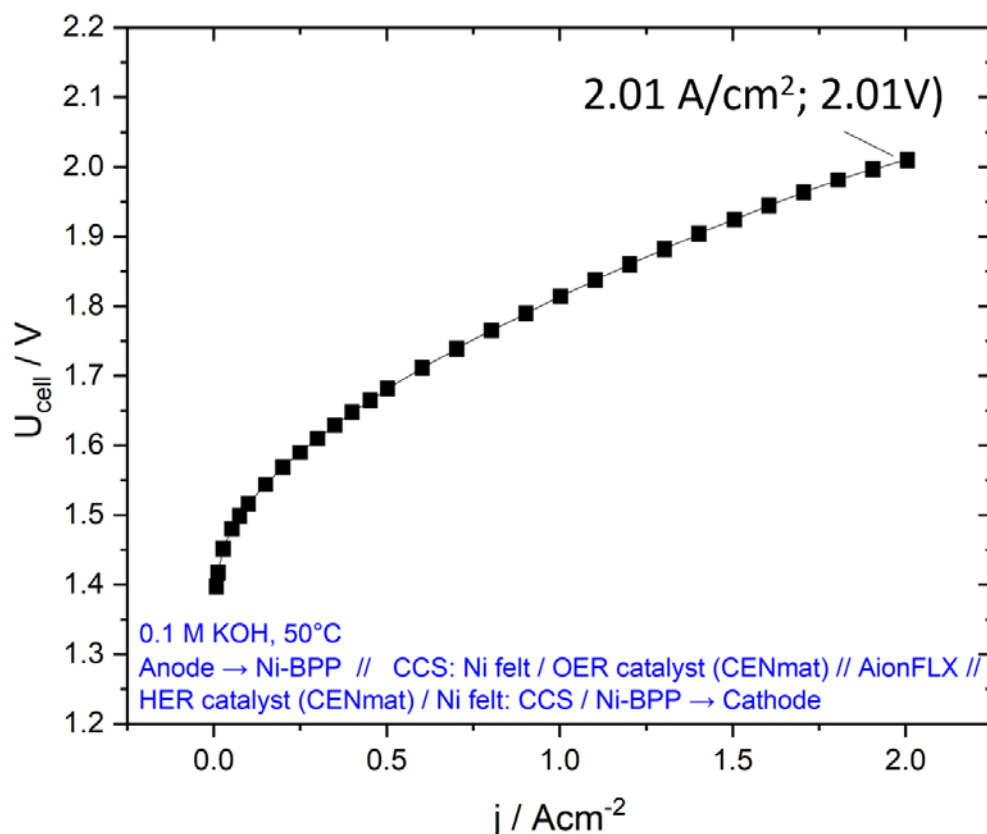
Good stability was recorded up to 330 hours (Fig. 10), with a degradation rate below 5 µV/h. This was observed considering that the cell reached a stable voltage approximately 11 hours after BoT (Beginning of Test) and maintained it until the last recorded point.

An increase in the decay rate was observed after the first stop (EIS + POL at 170 hours), which appears to be related to reversible losses. A complete recovery of performance was noted following the shutdown/startup cycle. Additionally, a partial voltage recovery was observed after partially refilling the KOH solution with pure water. Despite these issues, the MEA stability prior to the stop remained consistent and aligned with the project's target.
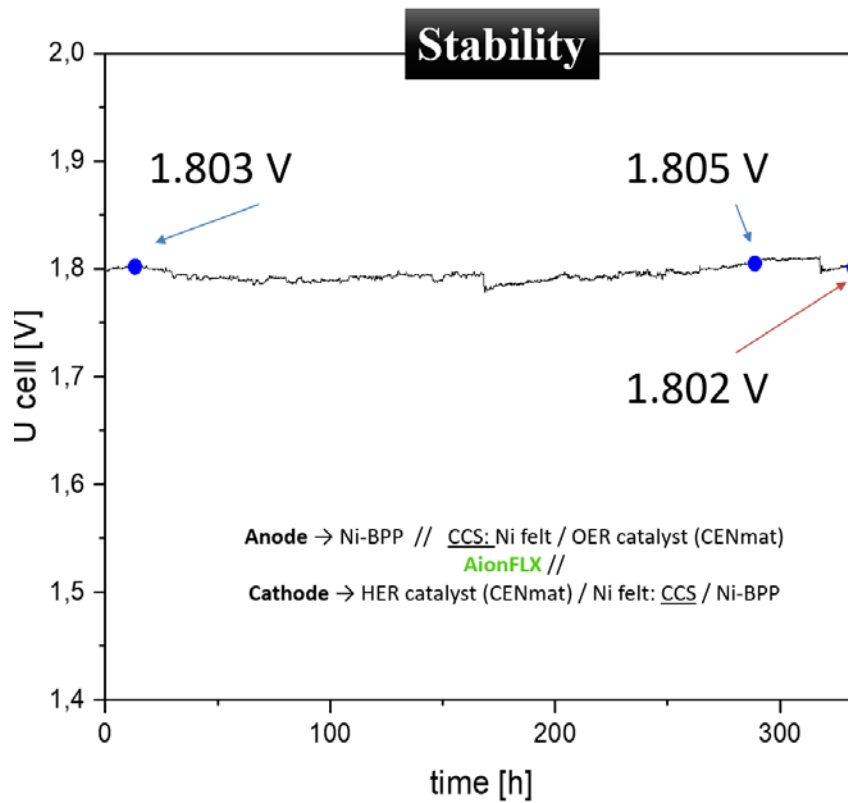
D3.1. Assessment of large area AMEL cells

Figure 10. Durability of AionFLX membrane in 0.1 M KOH and 50 °C.

Figure 11 shows the polarizations curve performed at BoT, after 170 hours and 330 hours. The results reveal an improvement of performance of cell after 170 h compared to the BoT. Anyway, the cell returned to the initial values at 330 hours.
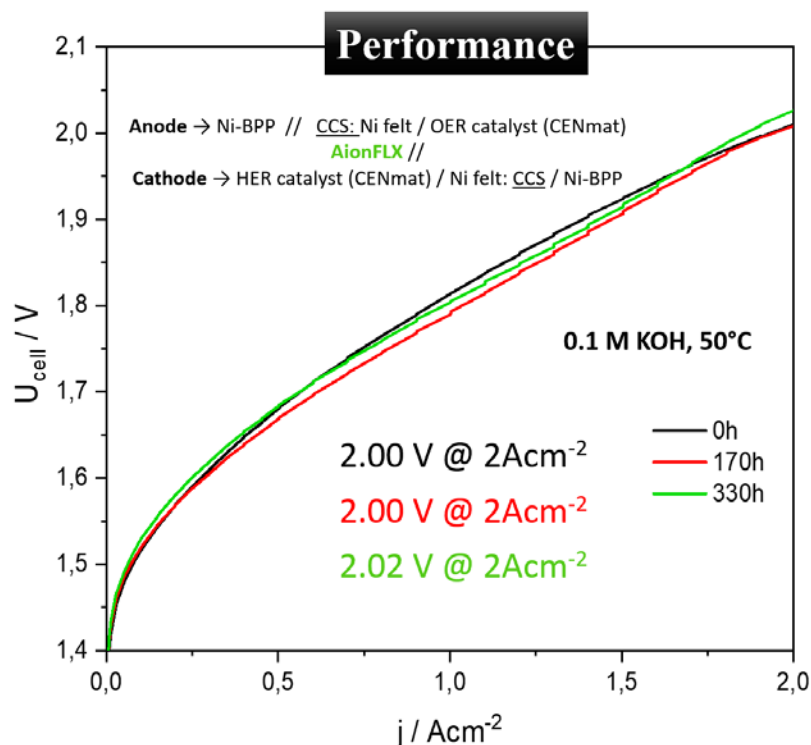
D3.1. Assessment of large area AMEL cells

Figure 11. Polarization curves performed in three points during the stability test of 330 hours.

3. Large area cell assessment at CNR

Based on the results and screening of active materials in a small single cell, the large-area cell was designed and manufactured. However, some changes were necessary to meet the project targets during the scale-up of the cell design. The goal is to validate the performance achieved in the single cell and understand how to improve the design for the short stack. A new architectural design was developed based on CNR's previous experience.

To minimize material waste during the manufacturing process of cell components such as PTL, membrane, and nickel grid, a square shape was chosen for the large cell area. This approach primarily aims to reduce the manufacturing costs of the components. A flow-field-free design was adopted to eliminate machining costs, enabling the use of inexpensive Ni current collectors. The final goal for the bipolar plate is to focus on nickel or Ni-coated steel as cost-effective materials with high conductivity and good corrosion resistance in alkaline conditions. However, steel materials are less resistant to high-concentration alkaline solutions compared to nickel.

The activities have been focused on:

- Design of large single cell to reduce the thickness of frame.
- Assessment of material tested in the small single cell.

Tests on the large single cell are starting as part of the short stack phase, but it was designed using cost-effective materials and a configuration that closely aligns with the final approach.

D3.1. Assessment of large area AMEL cells

3.1 Cell configuration

The cell features a flow-field-free design to reduce hardware and machining costs. However, to enhance the electrical contact between the PTL and the expended nickel grid and to provide better mechanical support to the membrane, an additional nickel component with denser porosity was incorporated.

The configuration of the large single cell area is shown in figure 12, which illustrates the position and structure of the components. The anode and cathode compartments each consist of three layers, in addition to the current collector.
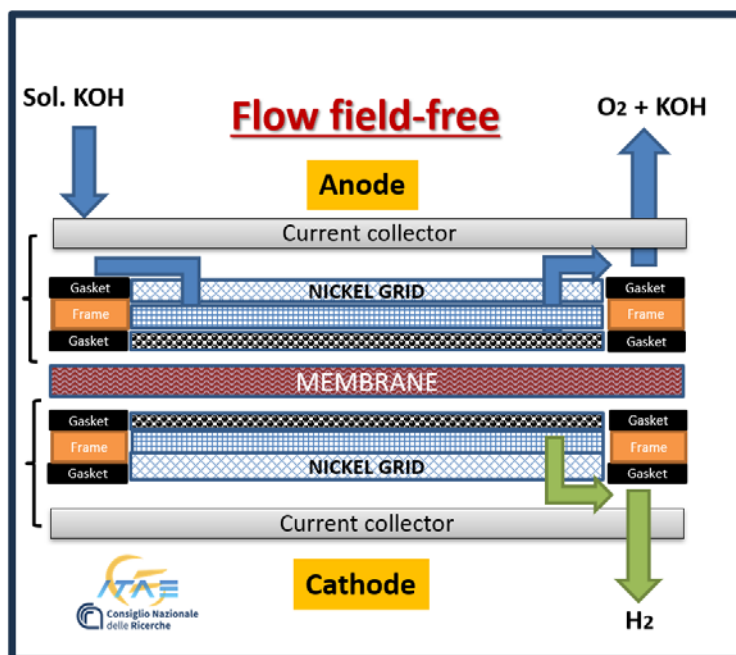

Figure 12. Large single cell configuration and components used.

3.2 Electrochemical test

- **Polarization Curves and GEIS Analysis**

Table 5 shows the configuration of the large cell area for the electrochemical tests. For these initial tests, the Piperion membrane was chosen due to issues encountered during tests with the small single cell. In subsequent tests, the improved membrane developed by CENmat will be used.

Table 5. Large cell area configurations with CENmat components

Large Cell area configurations				
	Catalyst/Material	**Loading/thickness**	**Ionomer**	**PTL**
Anode	OXYGN-N (CENmat)	Confidential (CENmat)	AionFLX (CENmat)	Nickel felt 450 µm (Bekaert)
Cathode	H2GEN-M (CENmat)	Confidential (CENmat)	AionFLX (CENmat)	Nickel felt 450 µm (Bekaert)
AEM Membrane	Piperion (commercial)	60 µm	/	/

D3.1. Assessment of large area AMEL cells

In figure 13, some pictures of large cell area are shown during the electrochemical tests. The tests were conducted feeding only the anode with a KOH solution 0.1M.
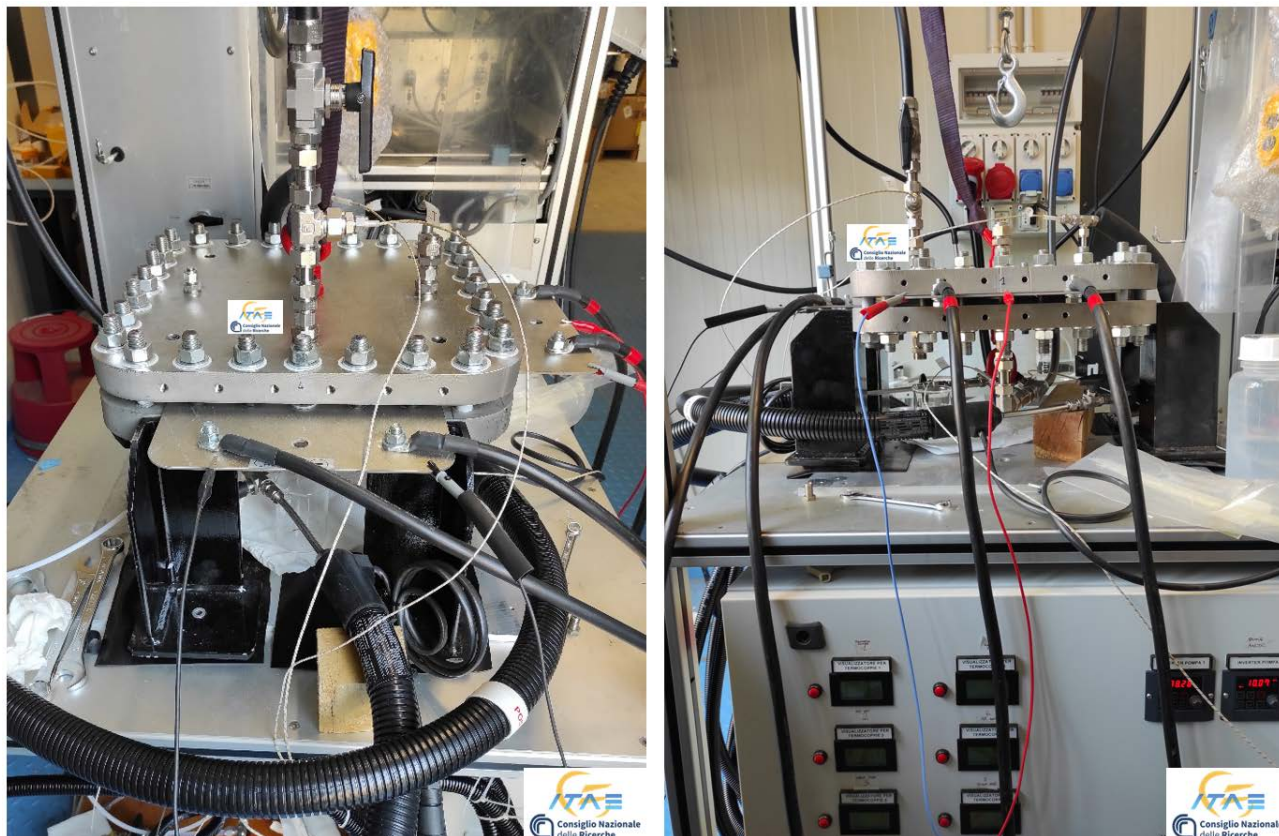

Figure 13. Pictures of large area single cell under testing at CNR.

Figure 14 shows a comparison of the polarization curves and GEIS results between the large area single cell and the small single cells tested with the Piperion (commercial) and AionFLX (CENmat) membranes. The large area cell exhibited similar behavior to the small single cell with the Piperion membrane at low current density but demonstrated improved performance at high current density. When compared with the small single cell utilizing the AionFLX membrane, the large area cell showed worse performance at low current density but better results at high current density. However, GEIS analysis revealed a higher series resistance for the large area cell at 0.1 A/cm² in both cases.

A performance slightly above 2 V (2.07 V) was achieved at 2 A/cm² for the large single cell area (designed 408 cm², restricted to 324 cm² to protect the membrane edges during electrochemical tests). Therefore, milestone MS 3a was also nearly achieved for the large area cell and could be fully reached by addressing certain diffusion-related issues. In table 6 is shown the faradaic efficiency calculated at four current densities with a mass flow meter.

In detail, the faradaic efficiency (η_F) was calculated by comparing the actual amount of hydrogen produced during electrolysis to the theoretical amount based on the total charge passed. The theoretical hydrogen production was determined using Faraday's law:

$$\text{Theoretical moles of } H_2 = I \cdot t/z \cdot F$$

D3.1. Assessment of large area AMEL cells

where *I* is the current (A), *t* is the time (s), z = 2 is the number of electrons per mole of hydrogen, and F=96,485 C/mol is Faraday's constant. The actual hydrogen production was measured using a gas flow meter and corrected to standard temperature and pressure (STP). The faradaic efficiency was then calculated as:

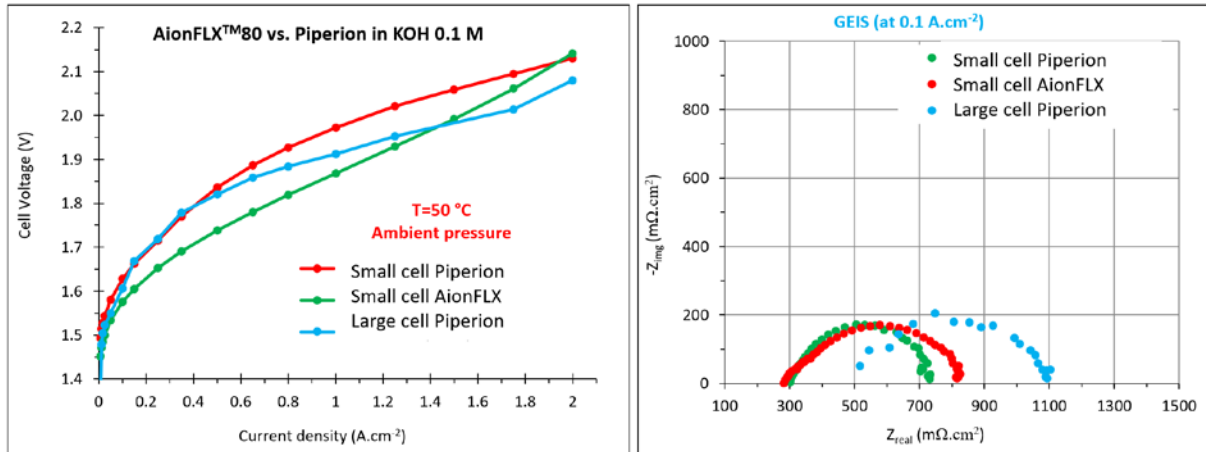$$\eta_F = (Actual\ moles\ of\ H_2)\ /\ (Theoretical\ moles\ of\ H_2) \cdot 100$$

Figure 14. Polarization curves and GEIS comparison at CNR between the large area single cell and small single cells.

Table 6. Faradaic efficiency at different current density for the large single cell area.

Faradaic efficiency for the Large single Cell	
Current density (A/cm^2)	Faradaic efficiency (%)
0.20	98.15
0.22	98.9
0.37	98.7

3.1 Durability test at CNR on Large area cell

To investigate the stability of the large-area single cell (≈400 cm2), a 110-hour test was conducted. The results demonstrated good stability, with a slight reduction in voltage over time. Two interruptions occurred during the test due to BoP issues (fig.15).

The first interruption happened at approximately 50 hours, during which the cell remained in warm recirculation for about 5 hours before restarting. The second break occurred around 100 hours, with a rest of 30 minutes.
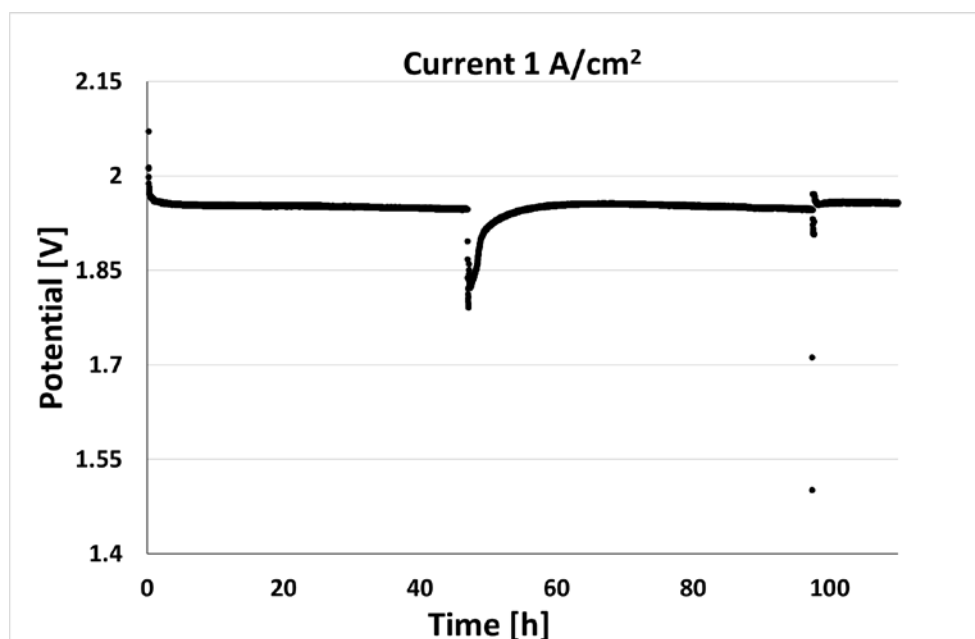
D3.1. Assessment of large area AMEL cells

Figure 15. Durability test at CNR on Large area cell.

4. Summary and conclusions

This report presents a systematic evaluation of small- and large-area single cells assembled with advanced Anion Exchange Membranes (AEMs) and catalyst-coated substrates (CCSs) for the optimization of large-area AMEL cell components. For the small cell, the study compares two cell configurations using CNR catalysts and two configurations with CENmat catalysts, focusing on the impact of using Ni felt (450 µm) versus carbon paper as the CCS in the cathode. Initial results revealed that the cell configuration using carbon paper as the PTL on the cathode side performed better than the Ni felt 450 µm configuration. The small single cell with carbon paper achieved a current density of 2 A/cm² at 1.98 V in a 1 M KOH solution, demonstrating the achievement of milestone 3a (2 A/cm² at <1.85-2 V/cell). However, due to the mechanical robustness and durability requirements for stack applications, the configuration with Ni felt on both anode and cathode sides was selected for further testing. Additionally, Long-term stability tests showed that cells with Ni felt on both the anode and cathode sides maintained more stable performance under continuous operation at 1 A.cm⁻² compared to configurations with carbon paper, which experienced higher degradation. Thus, the Ni felt 450 µm configuration was selected for further optimization.

Further studies explored the effect of KOH concentration on the Ni felt configuration. Cells operating in 1 M KOH demonstrated better performance at the beginning of the test (BoT) with lower cell voltages at given current densities and reduced resistance, as shown by both polarization curves and galvanostatic electrochemical impedance spectroscopy (GEIS). However, to meet operational goals, we aim to reduce KOH concentration to approximately 0.1 M to balance performance with material stability.

A comparative analysis of two AEMs, Piperion and AionFLX, highlighted additional performance and stability considerations. Polarization and GEIS data showed that AionFLX outperformed Piperion at BoT in both KOH 1 M and 0.1 M, with the polarization curves showing

D3.1. Assessment of large area AMEL cells

lower cell potentials, and the GEIS data showing lower charge transfer resistance and improved reaction kinetics.

Tests conducted with the large single cell area showed better performance than the small cell at high current densities and allowed reaching 2 A/cm² at a voltage of 2.07 V in a 0.1 M KOH solution. Milestone MS 3a has almost been reached for the large area cell and can be fully achieved by addressing specific diffusion-related challenges.

In conclusion, the study identifies a promising cell configuration with Ni felt on both electrodes and highlights the need to optimize membrane stability. This configuration lays the groundwork for developing robust, high-performance AEM large-area set up which will inform the fabrication of the short stack prototype (Deliverables 3.2 and 3.3) still to come in WP3, as well as stack design and development in WPs 4 and 5.

www.hyscale.eu